RSC Advances

ROYAL SOCIETY OF CHEMISTRY

www.rsc.org/advances

Simulation and Sensitivity Analysis of Transport in Asymmetric Hollow Fiber Membrane Permeators for Air Separation

Seyed Saeid Hosseini [a*], Sara Najari [a], Prodip K. Kundu [b], Nicolas R. Tan [c], Seyed Mehrdad Roodashti [a]

[a] Department of Chemical Engineering, Tarbiat Modares University

Tehran, Iran 14115-114

[b] Department of Chemical Engineering, University of Waterloo,

Waterloo, ON, Canada N2L 3G1

[c] Research & Development Dept., HOSSTECH Group,

Singapore 528844

[*] Corresponding author: S.S. Hosseini; Tel.: +98 21 82883335, Fax: +98 21 8288 4931.

E-mail address: saeid.hosseini@modares.ac.ir).

Abstract

Development of high performance membranes requires deep insights about the various design, fabrication and operational parameters involved in the process. In the present study, the influence of input parameters such as active fiber length, feed temperature, feed composition and feed pressure is investigated to analyze the efficiency of models for the separation of O_2/N_2 mixtures using asymmetric hollow fiber permeator. In addition, the effect of various non-idealities on membrane performance are studied, individually. Results reveal that in contrast to pressure, temperature changes has no influential effect on the concentrations of O_2 and N_2 at permeate and retentate streams. The influence of feed composition on the product purities is more significant compared to active fiber length. Moreover, analysis of non-ideal effects indicate that pressure changes and concentration polarization are the most significant non-idealities among other effects. Results of this investigation can effectively be used to find a comprehensive view about the impact of influential parameters and non-ideal effects on the membrane separation performance for O_2/N_2 separation application.

Key words

Membrane Permeator; Asymmetric Hollow Fiber; Sensitivity analysis; Modeling and Simulation; Air Separation

1. Introduction

The emergence of membrane technology since 80s has led to remarkable revolutions in the gas and vapor separation industry. Over the years, membrane technology has turned into one of the major competitors to the conventional gas separation technologies such as absorption, adsorption and cryogenic distillation. Modularized membranes with compact size, lower energy consumption and easy scale-up are now being developed and widely used for variety of gas separation applications including but not limited to natural gas dehydration and sweetening, air separation and hydrogen purification [1-4]. Undoubtedly, the advent of asymmetric membranes by the Loeb and Sourirajan [5] can be regarded as one of the leading breakthroughs that enabled obtaining membranes with more mechanical stability, high throughput (flux) and efficiency (selectivity) [6-8]. Accordingly, many research works and experiments have been carried out since then in order to design and fabricate high performance membranes [2, 3, 9-13].

One of the key techniques in design and development of high performance membranes has been through the employment of mathematical models and simulation studies. In fact, appropriate mathematical models can enable membrane manufacturers and process designers for finding opportunities that can be used for optimizing the process performance. In addition to the validity and accuracy, the ability to provide information about the trend of changes and variations in the input parameters and their respective effects on the behavior of the system and output parameters would be beneficial and of high importance [14-16]. This can be achieved through sensitivity analysis. In addition, sensitivity analysis can assist in determining the degree of the influence of the parameters and identifying those with the highest impact [17]. A considerable number of research studies have been carried out on the modeling and simulation of hollow fiber gas separation permeators; however, only limited studies have provided information about the effect

of involved parameters on the separation performance [18-21]. Pan and Habgood [22] developed mathematical models for the analysis of gas permeability in hollow fiber modules with significant pressure drop in the lumen-side. Their findings revealed that the performance of the membranes with narrow lumen can be significantly affected by the permeate pressure build-up inside the narrow fiber. This was attributed to the fact that the permeate to feed pressure ratio in hollow fibers was more sensitive to the variations of the permeate pressure than the feed pressure, particularly in the case of shell-fed configuration. Furthermore, for a given module and at certain recovery rate, an optimum permeate outlet pressure was found to minimize the membrane and permeate compression costs.

In another study [23], Pan developed mathematical models in order to study and evaluate the effect of various parameters on the gas separation performance of asymmetric permeators. The findings revealed that the porous support in the asymmetric structure plays an important role in the behavior of the membrane compared to that with symmetric structures. It was also shown that the permeate pressure build-up in the narrow channels of hollow fibers is strongly dependent on the feed-permeate flow pattern. The counter-current mode offered the lowest permeate pressure build-up but the feed flow was in the undesirable direction in relation to the permeate pressure build-up. The co-current pattern, on the other hand, had the desirable direction of feed flow relative to the permeate pressure build-up but the permeate pressure build-up could be excessive. In overall, the net effect of the permeate pressure build-up and the feed flow direction is that the feed-permeate flow pattern can have little effect on the membrane performance and that the counter-current pattern may not necessarily be the preferred operating mode.

In a subsequent study, Kundu et al. [24] developed mathematical models for analysis of high flux hollow fiber membranes and generated profiles for the residue and permeate flow rates, the

residue and permeate compositions, as well as the pressure build up along the fiber bore in order to investigate the effect of each parameter on the air separation performance. The results showed that the increase in feed pressure resulted in increase in permeation driving force for both components and consequently a higher stage-cut was achieved. On the other hand, permeate purity with respect to O_2 and retentate purity with respect to N_2 were decreased and increased respectively upon increase in stage-cut. Fattah et al. [25] developed mathematical models by taking into account the non-ideality of feed-side gas mixture at high pressure for the analysis of gas separation in permeators. The findings revealed that the non-ideal model estimated higher permeate enrichment, retentate depletion and membrane area but lower stage-cuts compared to the model developed based on ideal conditions. This was attributed to the decrease in permeation driving force across the membrane caused by reduction in fugacity coefficient at higher pressures. Stage-cut was increased upon increasing the pressure difference across the membrane; however, the permeate enrichment, retentate depletion and required membrane area were all decreased. Also Alpers et al. [26] developed both ideal and extended (by accounting fugacity coefficients) models to investigate the performance of high flux membrane for separation of organic vapors from air. They found that for a quaternary mixture of methane, ethane, propane, and n-butane, the membrane selectivity and the retentate mole fractions were almost comparable for both ideal and extended models having feed pressures of up to 15 bar. However, further increase in feed pressure resulted in deviation in between the ideal and extended models for predicting the membrane permeation and separation performance.

Mourgues and Sanchez [27] developed a mathematical model to investigate the effect of concentration polarization on the performance of hollow fiber gas separation membranes. They found that concentration polarization significantly affected the performance of the membranes

particularly those possessing selectivity of 100 and permeability (of the more permeable gas) exceeding 1000 GPU. In the case of temperature changes due to permeation, Rautenbach and Dahm [28] analyzed the influence of Joule-Thomson effect on the separation characteristics of membrane module used for both air separation and methane enrichment in landfill gas. They demonstrated that relatively large errors could happen if Joule-Thomson effect is not taken into account in the design of membrane permeators. Also, they indicated that the influence of Joule-Thomson effect could be pronounced upon increase in absolute values of activation energy for permeation. Safari et al. [29] presented two simple mathematical models to account for the dependence of membrane permeability and selectivity to temperature and pressure simultaneously. It was illustrated that the permeability was increased upon increase in temperature or decrease in pressure. On the other hand, they concluded that increase in both temperature and pressure resulted in the reduced selectivity. In addition, the effect of temperature on selectivity was more pronounced.

Despite the numerous studies carried out on modeling and simulation of the gas separation permeators, no specific study could be found that can provide deep insights to the effect and importance of influential parameters, membrane geometry and operational conditions on the separation performance. In continuation to the developments of various gas separation membranes [2, 3, 7, 9-12], the authors recently presented a useful methodology for mathematical modeling based on both ideal and non-ideal conditions for separation of binary gas mixtures [30]. The ideal model is developed based on the maximum possible assumptions and simplifications. On the other hand, the non-ideal model is developed by incorporating several realistic parameters to the ideal model including real gas behavior, temperature, pressure and

concentration dependence of gas viscosity as well as pressure changes on both sides of hollow fibers, concentration polarization, temperature changes due to permeation and temperature dependence of membrane permeance [30, 31]. The objective of the present study is to employ rigorous sensitivity analysis of the developed mathematical models to analyze the effect of module properties and process operational conditions on the membrane separation performance. The effect of variations in active fiber length, feed temperatures, feed pressures and feed compositions were the few important input parameters investigated and analyzed in details. Furthermore, the role and the extent of contribution of each non-ideal effect on the separation performance of the membrane was evaluated and presented in an exemplary case of a hollow fiber membrane permeator for air separation. The experimental data presented by Feng et al. [32] were used to accomplish the analyses for both ideal and non-ideal conditions. The findings can effectively be used for determination of the impact of influential parameters and non-ideal effects on the membrane separation performance for gas separation applications.

2. Simulation and Sensitivity Analysis Procedures

Simulation is a powerful tool since it can provide valuable information for the design, optimization and economics of various separation processes including membrane permeators with minimum cost and effort [24, 33]. Accordingly, both ideal and non-ideal conditions were modeled in our previous study [30]. The models used for the simulation of the hollow fiber membrane separator are comprehensive enough to investigate the influence of the key parameters on the separation performance via sensitivity analysis.

Sensitivity analysis was carried out using *brute force* technique [17]. This technique is suitable mostly for relatively simple models with limited equations that can be solved with less

complexity involved. According to this technique, a selected input parameter is changed within a certain range while keeping other parameters constant in order to realize the degree of the sensitivity of the output parameter to the selected variable one. These parameters are related to the properties of the feed, permeate and retentate streams, the flow and module configurations, as well as the properties of the membrane material and the governing transport mechanisms involved [30]. Accordingly, active fiber length, feed temperature, pressure along with feed composition are selected as the main parameters.

The active fiber length represents the physical geometry of the membrane while temperature, pressure and composition of the feed are all associated to the process operational conditions. The mole fraction of the more permeable component in the permeate as well as the mole fraction of the less permeable component in the retentate streams are considered as the output parameters. These output parameters were taken as the key indices for evaluation of the separation performance of the hollow fiber module for air separation. A schematic of the geometry and flow configuration of the module comprised of the asymmetric hollow fiber membranes used for the simulation and sensitivity analysis is presented in Fig.1. In addition, the specifications of the module and process conditions which used for the sensitivity analysis are provided in Table 1.

Fig. 1

Table 1

3. Results and Discussions

3.1. The effects of active fiber length

The effect of active fiber length on the process performance was investigated for hollow fibers having 5 to 20 cm length whilst other parameters such as feed temperature, pressure and composition remained constant. Fig. 2 demonstrates the results of simulation and sensitivity

analysis carried out using both ideal and non-ideal models based on the mole fractions of O_2 (i.e., more permeable component) and N_2 (i.e., less permeable component) at the outlet of permeate and retentate streams, respectively. The corresponding stage-cuts for both models are provided for each active fiber length beneath the corresponding value.

Figure 2

The simulations considering non-ideal model show that an increase in the active fiber length from 5 to 20 cm led to 18.7% decrease (from 0.459 to 0.374) in the mole fraction of O_2 in the permeate stream whereas the mole fraction of N_2 in the retentate increased by 10.3% (from 0.829 to 0.913). A longer fiber can be translated to the larger membrane area available for the permeation of gas molecules and consequently higher stage-cuts. Higher stage-cut causes passage of a larger amount of gas through the membrane along the extended fiber length. Upon increase in fiber length, the retentate stream is gradually depleted from the more permeable component (i.e., oxygen) and enriched with less permeable component (i.e., nitrogen) and this extended fiber length provides more opportunity for the permeation of nitrogen through the membrane compared to the smaller fiber length. Hence, the permeate side becomes diluted with the less permeable component and purity of more permeable component in the permeate side decreases. In other words, a trade-off relationship exists between the product recovery and purity [34]. Therefore, due to depletion of oxygen from feed stream, higher stage-cuts are achieved with less enriched permeates [4]. It was interesting to note that the trends of simulation results by both ideal and non-ideal models were comparable, albeit higher purities of O_2 and N_2 were predicted by the ideal model than that of the non-ideal model for both the permeate and the retentate streams, respectively. Accordingly, the ideal model predictions were about 1.7% and 1% higher in the case of O_2 and N_2 purities for the fiber with length of 0.2 m. This can be

attributed to the cumulative declining contribution of non-ideal effects accounted for in the non-ideal model.

The effects of active fiber length on the purity of permeate and retentate streams at different feed compositions predicted by non-ideal model are illustrated in Fig. 3. The results implied that increase in the active fiber length results in the reduction in the purity of the oxygen at the permeate side while increase in the nitrogen purity in the retentate side. The trend was almost similar for the product quality in the permeate stream. However, the results suggested that the purity of nitrogen in the retentate side increased more by an increase in the active fiber length for feed gas with higher oxygen content. As earlier mentioned, larger membrane area provides higher recovery of O_2 in permeate stream and lower recovery of N_2 in the retentate stream. Increasing O_2 concentration in the feed stream has a synergetic effect on reducing the recovery of N_2 in the retentate and as a result of trade-off between recovery and purity, the concentration of N_2 in the retentate increases sharply.

Figure 3

3.2. The Effect of Feed Composition

The effect of feed composition on the process performance was investigated by varying the mole fraction of O_2 in the feed (i.e., in the range of 0.1 to 0.4) whilst other parameters such as active fiber length, feed temperature and pressure were kept constant. Fig. 4 demonstrates the results of the sensitivity analysis for both the ideal and non-ideal models based on the mole fractions of O_2 and N_2 at the outlet of permeate and retentate streams, respectively, with fibers having active lengths of 0.1 and 0.2 m.

Figure 4

The findings suggest that by increasing the concentration of the more permeable component (i.e., O_2) in the feed stream, the concentration of O_2 increases in permeate outlet as a result of increase in the permeation driving force for O_2 while the permeation driving force for N_2 is reduced. Therefore, considering the non-ideal model, more O_2 permeates through the same membrane area and the purity of O_2 in the permeate stream increases by about 0.43 and 0.38 for the modules containing fibers with an active length of 0.1 and 0.2 m, respectively. Moreover, according to the ideal model, since the concentration of O_2 in retentate increases, the purity of N_2 in retentate decreases by nearly 0.2 and 0.1 as can be observed in Fig. 4 (b) for the length of 0.1 and 0.2 m, respectively. As discussed previously, at any specified feed composition, higher recovery and hence lower O_2 and higher N_2 purities are obtained for a longer fiber. In addition, by increasing the concentration of O_2 in the feed stream, the prediction by ideal model deviates more from that of non-ideal model. Accordingly, the purity of N_2 decreased by 0.21 and 0.14 for the 0.1 and 0.2 m active fiber length, respectively, due to taking into consideration of the associated non-ideal effects which is more realistic and practical. The non-ideal conditions comprise of concentration polarization, pressure changes in two sides of membrane and Joule-Thomson effect. The purity of O_2 in permeate and N_2 in retentate streams as a function of mole fraction of O_2 in feed at different active fiber lengths are illustrated in Fig. 5.

Figure 5

It is observed in Fig. 5 (a) that feed with higher oxygen content results in permeate streams with high purity oxygen at any specified fiber length. For example, increase in oxygen mole fraction from 0.1 to 0.4 in the feed led to the enhancement of oxygen purity in the permeate stream from 0.260 to 0.699 for the fibers having 0.05 m active length. The enhancement of oxygen purity in the permeate was about 181.5% for the fibers with 0.2 m active length. This can be ascribed to

the fact that since the membrane is semi-permeable and oxygen selective, increasing O_2 concentration in feed stream facilitates the opportunity and provides more driving force for the permeation of more O_2 molecules through the membrane. In other words, the findings indicate that both increase in the mole fraction of oxygen in the feed as well as using fibers with shorter active length can simultaneously achieve permeate with high purity of oxygen. On the other hand, an increase in oxygen content in the feed results in the decrease in the nitrogen mole fraction in the retentate stream as shown in Fig. 5 (b). The nitrogen mole fraction in the retentate stream reduced from 0.917 to 0.660 equivalent to a 27.95% decrease upon increase in the oxygen mole fraction from 0.1 to 0.4 for the fibers having 0.05 m active length. The reduction was about 14.24% in case of fibers with the active length of 0.2 m. This suggests that obtaining a specified purity of products with a longer fiber requires a higher concentration of O_2 in the feed. This can be also inferred from Fig. 6 in which the predicted purity of more permeable component is presented as functions of both fiber length and O_2 mole fraction in feed. Moreover, Fig. 6 shows that purity is more affected by the feed composition than active fiber length.

<div align="center">Figure 6</div>

3.3. The Effect of Feed Temperature

The effect of feed temperature on the process performance was investigated by varying the feed temperature in the range of 275.15 to 365.15 K whilst other parameters such as active fiber length, feed composition and pressure were kept constant. Fig. 7 demonstrates the results of simulation and sensitivity analysis carried out using both ideal and non-ideal models based on the mole fractions of O_2 and N_2 at the permeate and retentate streams, respectively, for the fibers having active lengths of 0.1 and 0.2 m.

Figure 7

The results showed that considering ideal model and regardless of the active fiber length, the changes in the process temperature do not affect the composition at neither permeate nor retentate streams due to nearly ideal behavior of the considered binary system (i.e., low fugacity coefficients) and also low feed pressure (approximately 8 bar). However, non-ideal model simulation results showed that oxygen content in the permeate stream as well as nitrogen content in the retentate stream were reduced gradually upon increase in temperature. However, the magnitude of changes in the composition at the retentate stream upon variation of temperature was less compared to that in the permeate outlet. For instance, the purity of N_2 decreased from 0.94% to 1.1% while that of O_2 decreased from 1.2% to 2.7% at the length of 0.2 m. This can be due to the enhanced diffusion coefficients of both components which led to the increased stage-cuts knowing that higher temperatures leads to increased permeability and reduced selectivity [20]. Earlier findings have demonstrated that the larger stage-cut can cause larger changes in the temperature [18]. On the other hand, the decrease in the purity of N_2 in retentate stream (0.18%) is less considerable which may be due to the fact that feed stream is less affected by the non-ideal effects.

The effects of feed temperature on the purity of O_2 and N_2 in permeate and retentate streams at different pressures are depicted in Fig. 8. It could be noted that the declining trends for both oxygen at the permeate and nitrogen at the retentate streams were almost similar for all the pressure ranges investigated. However, in overall, the declining trend of nitrogen in the retentate stream was very negligible. This may be due to the increase in the recovery and in turn stage-cuts accompanied with the decrease in retentate flow rate as can be seen in Fig. 9.

Figure 8

Figure 9

3.4. The Effect of Feed Pressure

The effect of feed pressure on the process performance was investigated by variation in the feed pressure in the range of 5 to 20 bar whilst other parameters such as active fiber length, feed composition and temperature remained constant. Fig. 10 demonstrates the effect of feed pressure variation for both the ideal and non-ideal models on the mole fractions of O_2 and N_2 at the outlet of permeate and retentate streams, respectively, for the fibers having active lengths of 0.1 and 0.2 m.

Figure 10

It could be observed that increase in the feed pressure had increasing effect on the oxygen content in the permeate outlet up to 10 bar whereas further increase in the pressure had declining effect. Accordingly, the highest O_2 purity was achieved at 10 bar.

Upon increase in the feed pressure, O_2 purity increased until reaching a maximum at around 0.468 and 0.437 for the length of 0.1 and 0.2 m, respectively. While further increase in pressure reduces O_2 Purity in permeate stream. In fact, at low pressures competitive sorption of components is dominant which results in reducing the permeance. As pressure increases driving force for mass transfer increases due to the augmented pressure difference across membrane. Therefore, N_2 passage through membrane is also increased by 10.59% and 16.70% for the length of 0.1 and 0.2 m, respectively, and consequently O_2 concentration in permeate is decreased (Fig. 10 (a)). Moreover, it can be observed that at longer fiber length maximum purity occurs at lower pressures. This may be due to more area available for the permeation of components which

provides higher permeation rates for both components. This is equivalent to higher stage-cut and lower O_2 purity. Besides, more O_2 passage through membrane results to less O_2 in retentate which in turn increases N_2 concentration in retentate stream (Fig. 10 (b)).

According to Fig. 10, the ideal model predicts higher purities for both O_2 and N_2 compared to the non-ideal model which arises from the effects of non-idealities. Accordingly, maximum purity of O_2 occurred at 0.479 and 0.445 for the length of 0.1 and 0.2 m where purity of N_2 increased by 11.59% and 17.26% respectively.

Fig. 11 represents the influence of pressure on the purities of O_2 in permeate and N_2 in retentate at different temperatures. It is observed that permeation of O_2 is much more affected by temperature compared to N_2. As temperature increases, purity of O_2 decreases, however, purity of N_2 only slightly decreases. This may be due to the fact that retentate flow is not considerably subjected to Joule-Thomson or concentration polarization phenomena since it does not pass through the membrane. Moreover, it can be also inferred that temperature has no significant effect on the trends of purities versus pressure since the maximum purity of O_2 and also the slope of change of N_2 purity remained unchanged.

Figure 11

3.5. Determination and analysis of the contribution of non-ideal effects

In design and analysis of membrane permeators, it is very important to determine the most influential non-ideal effects on the separation performance of membrane module. Accordingly, each of these effects applied in the formulation of simple model individually. The most

important parameters which were affected by considering the non-ideal effects were calculated and presented in Table 2.

Accordingly, Reynolds number in permeate stream is less than 2100, consequently, the assumption of laminar flow in fibers is valid. Also, these data justify that by increasing the feed pressure, pressure drop in feed stream decreases while pressure build-up in the permeate stream, temperature difference across membrane and the index of concentration polarization increase.

Table 2

The predictions of both ideal and non-ideal models for mole fractions of O_2 (i.e., more permeable component) and N_2 (i.e., less permeable component) at the outlet of permeate and retentate streams versus normalized length at various pressures are illustrated in Fig. 12. It can be observed that purity of O_2 in permeate stream decreases while that of N_2 in retentate increases as the normalized fiber length increases. This may be due to the fact that as O_2 permeates through the membrane, the driving force of permeation decreases along the fiber and the concentration of more permeable gas reduces in the feed stream. In addition, the slope of changes in the purities along the normalized fiber length increases as pressure increases. As pressure increases, the driving force for the permeation of both components increases due to the increase in the pressure difference across the membrane. However, since feed is rich in N_2, a great portion of permeated molecules are N_2 and therefore, purity of O_2 in the permeate decreases sharply at higher pressures. This is an indication of steeper reduce in driving force and hence the purity of N_2 in retentate increases faster. In addition, at low pressure, i.e., 5 bar, non-ideal model predicts lower purity for both O_2 and N_2. However, as pressure increases predictions of non-ideal model overtake those of ideal model. This occurs at shorter active fiber length as pressure increases.

Figure 12

In order to investigate the influence of non-ideal effects on the separation performance of hollow fiber, each effect was considered in the ideal model individually as displayed in Figs. 13-15.

Figure 13

It could be observed that the effect of pressure changes on both sides and concentration polarization are the most influential non-ideal effects among others. Accounting for the pressure changes leads the positive deviation from the predictions of ideal model. This may be due to the fact that pressure build-up in permeate stream and negligible pressure loss in feed stream lead to a decrease in the pressure difference across the membrane and hence the driving force of both components decreases. It seems that this decrease is more considerable for N_2 permeation which results in an increase in O_2 purity in permeate stream compared to ideal model predictions. In contrast, accounting for the effect of concentration polarization, results to lower product purity compared to the predictions of ideal model. Clearly, concentration polarization negatively influences the separation performance of the membrane module as a result of hindering the permeation of more permeable gas through membrane due to the accumulation of less permeable gas on the surface of fiber walls. Therefore, it is obvious to obtain less product purities than those of ideal model. The index of concentration polarization which is an indication of the extent of concentration polarization is presented in Table 2 and defined as follows [21]:

$$I_{CP} = 1 - \frac{x_{sa}}{x_a} \tag{1}$$

Where x_{sa} and x_a represent mole fractions of more permeable component on the surface and in the feed-side.

In addition, it can be observed that the curve depicting Joule-Thomson effect overlaps with the curve showing ideal condition in both O_2 and N_2 cases. Therefore, it can be inferred that permeability of components are not affected remarkably by temperature. Besides, it can be

observed that the behavior of O_2 (Fig. 13 (a)) is less near the real gas behavior compared to that of N_2 (Fig. 13 (b)) which may be due to lower fugacity coefficient of O_2 compared to that of N_2 in feed stream (Table 2).

Although the mentioned non-ideal effects seem to affect the product purities at higher pressures, it can be observed that the behavior of both components were less affected by the non-ideal effects (Figs. 14 and 15).

Figure 14

Figure 15

4. Conclusions

Following the previous part of this study, the sensitivity analysis for some important input parameters of the developed binary models (ideal and non-ideal) was performed and the extent of variation of each parameter was investigated, individually. Also the effect of non-idealities on the separation performance of hollow fiber membrane module were studied. Results confirmed that, using longer fibers led to lower O_2 purity and higher N_2 purity in permeate and retentate streams, respectively, due to higher stage-cuts. In addition, it was concluded that temperature had no influential impact on the product purities. However, variation in feed pressure considerably influenced the membrane separation performance. Accordingly, at low feed pressures purity of products increased due to higher driving force while further increase in pressure led to reduction in purities as a result of increase in recovery and therefore stage-cut. Besides, the influence of feed composition was of paramount significance in evaluating the membrane performance. It was concluded that using a feed stream richer in O_2 led to higher O_2 purity in permeate and lower N_2 purity in retentate due to the increased driving force for O_2 permeation. Moreover, the

influence of feed composition was found to be more significant than the effect of fiber length on the purity of more permeable component. Analysis of the non-ideal effects showed that the pressure changes at both sides and the concentration polarization were the most important non-ideal effects among others. Pressure changes led to lower pressure difference across membrane and hence lower driving force for permeation of less permeable component which led to positive deviation from simple model. However, concentration polarization negatively influenced the separation performance of membrane module by decreasing the purity of more permeable component. Results of this comprehensive analysis can be effectively employed to give a better understanding about the influence of important parameters and also non-ideal effects on the separation performance of hollow fiber membranes for O_2/N_2 separation.

Acknowledgements

References

[1] Y. Xiao, B.T. Low, S.S. Hosseini, T.S. Chung, D.R. Paul, The strategies of molecular architecture and modification of polyimide-based membranes for CO2 removal from natural gas—A review, Progress in Polymer Science, 34 (2009) 561-580.
[2] S.S. Hosseini, T.S. Chung, Carbon membranes from blends of PBI and polyimides for N2/CH4 and CO2/CH4 separation and hydrogen purification, Journal of Membrane Science, 328 (2009) 174-185.
[3] S.S. Hosseini, M.M. Teoh, T.S. Chung, Hydrogen separation and purification in membranes of miscible polymer blends with interpenetration networks, Polymer, 49 (2008) 1594-1603.
[4] M. Tamaddondar, H. Pahlavanzadeh, S. Saeid Hosseini, G. Ruan, N.R. Tan, Self-assembled polyelectrolyte surfactant nanocomposite membranes for pervaporation separation of MeOH/MTBE, Journal of Membrane Science, 472 (2014) 91-101.

[5] L. Sidney, S. Srinivasa, Sea Water Demineralization by Means of an Osmotic Membrane, in: Saline Water Conversion?II, AMERICAN CHEMICAL SOCIETY, 1963, pp. 117-132.

[6] M. Askari, T. Yang, T.-S. Chung, Natural gas purification and olefin/paraffin separation using cross-linkable dual-layer hollow fiber membranes comprising β-Cyclodextrin, Journal of Membrane Science, 423–424 (2012) 392-403.

[7] S.S. Hosseini, N. Peng, T.S. Chung, Gas separation membranes developed through integration of polymer blending and dual-layer hollow fiber spinning process for hydrogen and natural gas enrichments, Journal of Membrane Science, 349 (2010) 156-166.

[8] N. Peng, N. Widjojo, P. Sukitpaneenit, M.M. Teoh, G.G. Lipscomb, T.-S. Chung, J.-Y. Lai, Evolution of polymeric hollow fibers as sustainable technologies: Past, present, and future, Progress in Polymer Science, 37 (2012) 1401-1424.

[9] S.S. Hosseini, Y. Li, T.-S. Chung, Y. Liu, Enhanced gas separation performance of nanocomposite membranes using MgO nanoparticles, Journal of Membrane Science, 302 (2007) 207-217.

[10] S.S. Hosseini, M.R. Omidkhah, A. Zarringhalam Moghaddam, V. Pirouzfar, W.B. Krantz, N.R. Tan, Enhancing the properties and gas separation performance of PBI–polyimides blend carbon molecular sieve membranes via optimization of the pyrolysis process, Separation and Purification Technology, 122 (2014) 278-289.

[11] V. Pirouzfar, S.S. Hosseini, M.R. Omidkhah, A.Z. Moghaddam, Modeling and optimization of gas transport characteristics of carbon molecular sieve membranes through statistical analysis, Polymer Engineering & Science, (2013) n/a-n/a.

[12] V. Pirouzfar, A.Z. Moghaddam, M.R. Omidkhah, S.S. Hosseini, Investigating the effect of dianhydride type and pyrolysis condition on the gas separation performance of membranes derived from blended polyimides through statistical analysis, Journal of Industrial and Engineering Chemistry, (2013).

[13] S.S. Hosseini, T.S. Chung, Polymer blends and carbonized polymer blends, in, US Patent 8,623,124, 2014.

[14] S. Sundaramoorthy, G. Srinivasan, D.V.R. Murthy, An analytical model for spiral wound reverse osmosis membrane modules: Part II — Experimental validation, Desalination, 277 (2011) 257-264.

[15] W.B. Krantz, A.R. Greenberg, D.J. Hellman, Dry-casting: Computer simulation, sensitivity analysis, experimental and phenomenological model studies, Journal of Membrane Science, 354 (2010) 178-188.

[16] S. Najari, S.S. Hosseini, M. Omidkhah, N.R. Tan, Phenomenological modeling and analysis of gas transport in polyimide membranes for propylene/propane separation, RSC Advances, 5 (2015) 47199-47215.

[17] J.W. Chinneck, Practical Optimization: a Gentle Introduction, in, Carleton University, Ottawa, Canada, 2000.

[18] H. Gorissen, Temperature changes involved in membrane gas separations, Chemical Engineering and Processing: Process Intensification, 22 (1987) 63-67.

[19] G. He, Y. Mi, P. Lock Yue, G. Chen, Theoretical study on concentration polarization in gas separation membrane processes, Journal of Membrane Science, 153 (1999) 243-258.

[20] M. Scholz, T. Harlacher, T. Melin, M. Wessling, Modeling Gas Permeation by Linking Nonideal Effects, Industrial & Engineering Chemistry Research, 52 (2012) 1079-1088.

[21] R. Wang, S.L. Liu, T.T. Lin, T.S. Chung, Characterization of hollow fiber membranes in a permeator using binary gas mixtures, Chemical Engineering Science, 57 (2002) 967-976.

[22] C.Y. Pan, H.W. Habgood, Gas separation by permeation Part II: Effect of permeate pressure drop and choice of permeate pressure, The Canadian Journal of Chemical Engineering, 56 (1978) 210-217.

[23] C.Y. Pan, Gas separation by permeators with high-flux asymmetric membranes, AIChE Journal, 29 (1983) 545-552.

[24] P.K. Kundu, A. Chakma, X. Feng, Simulation of binary gas separation with asymmetric hollow fibre membranes and case studies of air separation, The Canadian Journal of Chemical Engineering, 90 (2012) 1253-1268.

[25] K.A. Fattah, S.M. Hamam, G. Al-Enezi, H.M. Ettoueny, R. Hughes, A nonideal model for analysis of gas separation permeators, Journal of Membrane Science, 65 (1992) 247-257.

[26] A. Alpers, B. Keil, O. Lüdtke, K. Ohlrogge, Organic Vapor Separation: Process Design with Regards to High-Flux Membranes and the Dependence on Real Gas Behavior at High Pressure Applications, Industrial & Engineering Chemistry Research, 38 (1999) 3754-3760.

[27] A. Mourgues, J. Sanchez, Theoretical analysis of concentration polarization in membrane modules for gas separation with feed inside the hollow-fibers, Journal of Membrane Science, 252 (2005) 133-144.

[28] R. Rautenbach, W. Dahm, Gas permeation — module design and arrangement, Chemical Engineering and Processing: Process Intensification, 21 (1987) 141-150.

[29] M. Safari, A. Ghanizadeh, M.M. Montazer-Rahmati, Optimization of membrane-based CO2-removal from natural gas using simple models considering both pressure and temperature effects, International Journal of Greenhouse Gas Control, 3 (2009) 3-10.

[30] S.S. Hosseini, S.M. Roodashti, P.K. Kundu, N.R. Tan, Transport Properties of Asymmetric Hollow Fiber Membrane Permeators for Practical Applications: Mathematical Modelling for Binary Gas Mixtures, The Canadian Journal of Chemical Engineering, 93 (2015) 1275-1287.

[31] S.S. Hosseini, W.B. Krantz, S.M. Roodashti, A Comprehensive Model for Gas Permeation and Separation in Asymmetric Hollow Fiber Membranes Considering Non-ideal Effects, in: AIChE Annual Meeting, San Francisco, California, Unites States, 2013.

[32] X. Feng, J. Ivory, V.S.V. Rajan, Air separation by integrally asymmetric hollow-fiber membranes, AIChE Journal, 45 (1999) 2142-2152.

[33] S.P. Kaldis, G.C. Kapantaidakis, G.P. Sakellaropoulos, Simulation of multicomponent gas separation in a hollow fiber membrane by orthogonal collocation — hydrogen recovery from refinery gases, Journal of Membrane Science, 173 (2000) 61-71.

[34] R.M. Smith, Chemical Process: Design and Integration, Wiley, 2005.

Retentate

Feed

Permeate

Direction of Feed Flow

Shell-side

Dense layer

Porous layer

Direction of Permeate Flow

Lumen-side

L

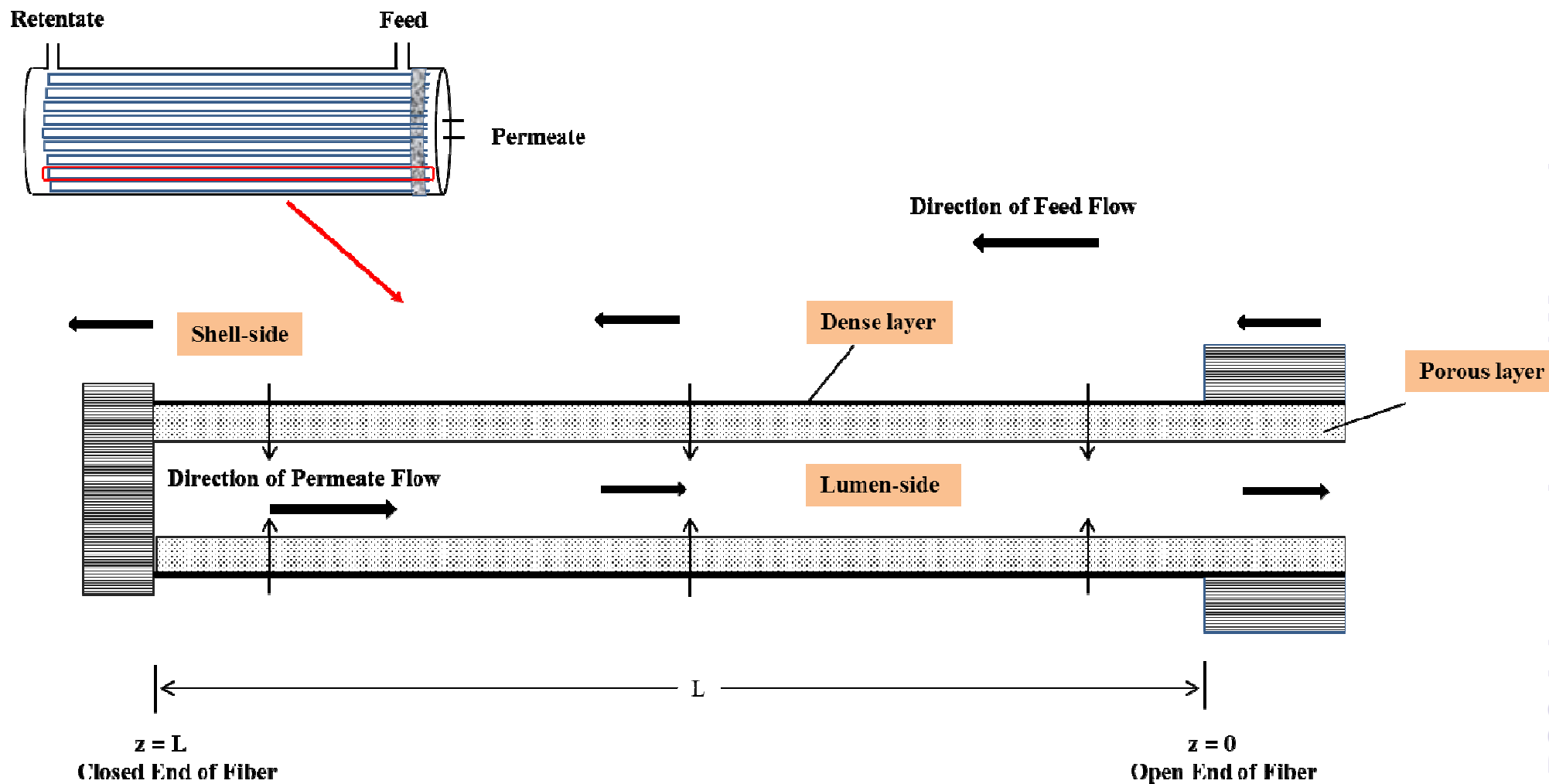z = L
Closed End of Fiber

z = 0
Open End of Fiber

Fig. 1. The geometry and flow configuration of the membrane permeator module and hollow fiber membranes inside used for simulation and sensitivity analysis.
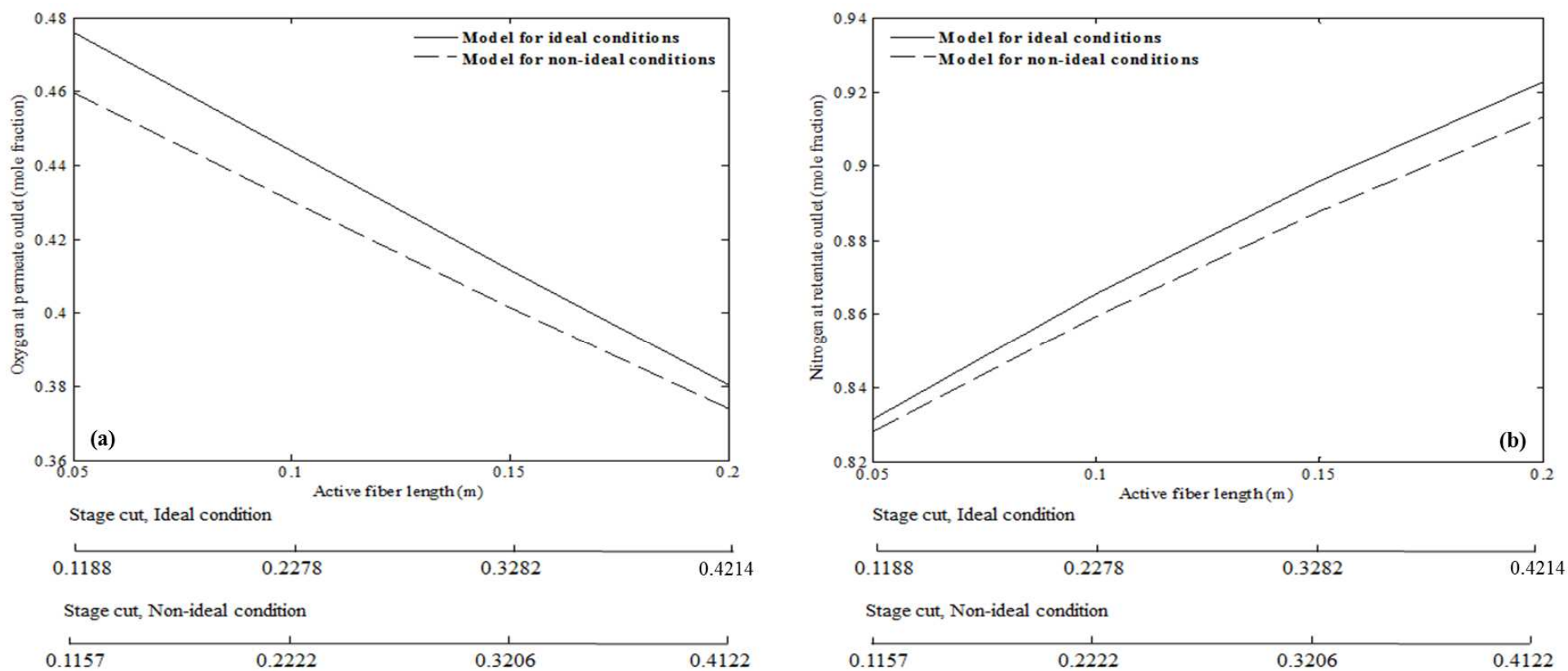
Figure 2. The effect of active fiber length on the products purity a) O_2 mole fraction in permeate stream b) N_2 mole fraction in retentate stream. (Testing conditions are provided in Table 1)
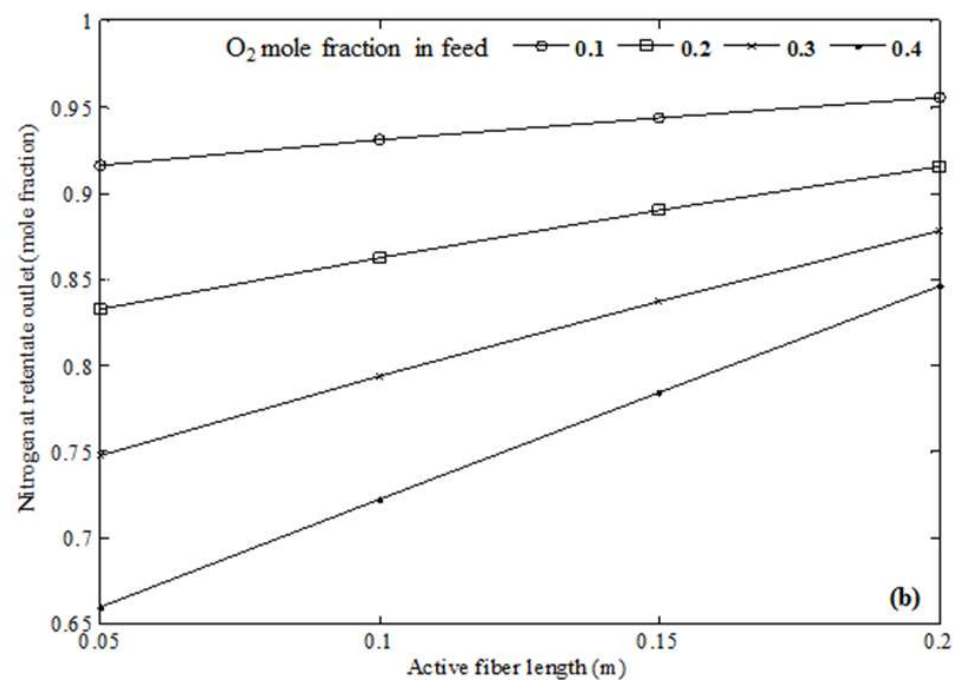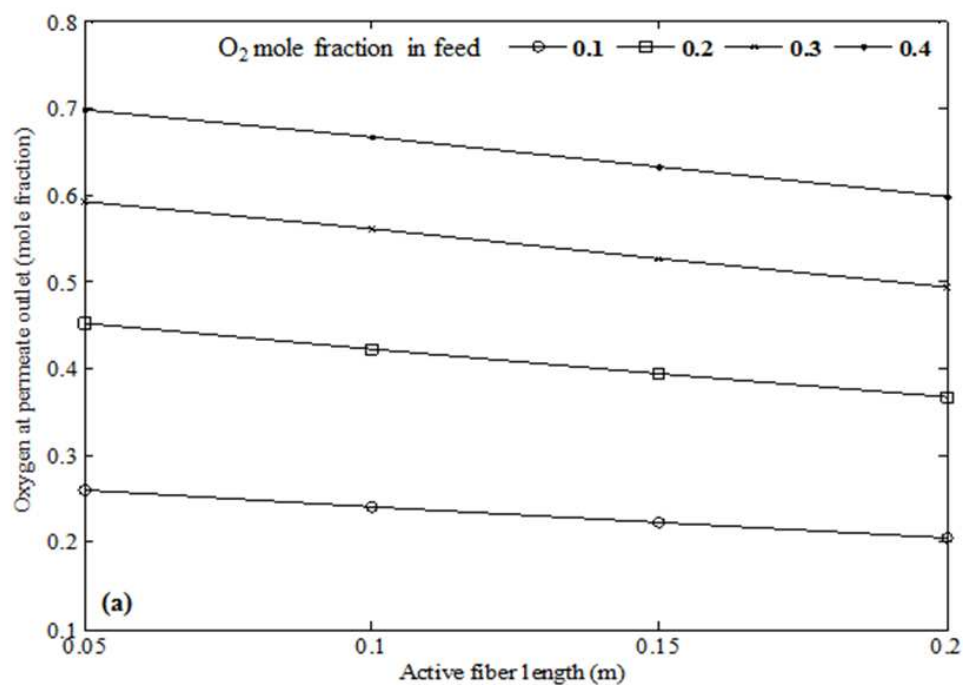
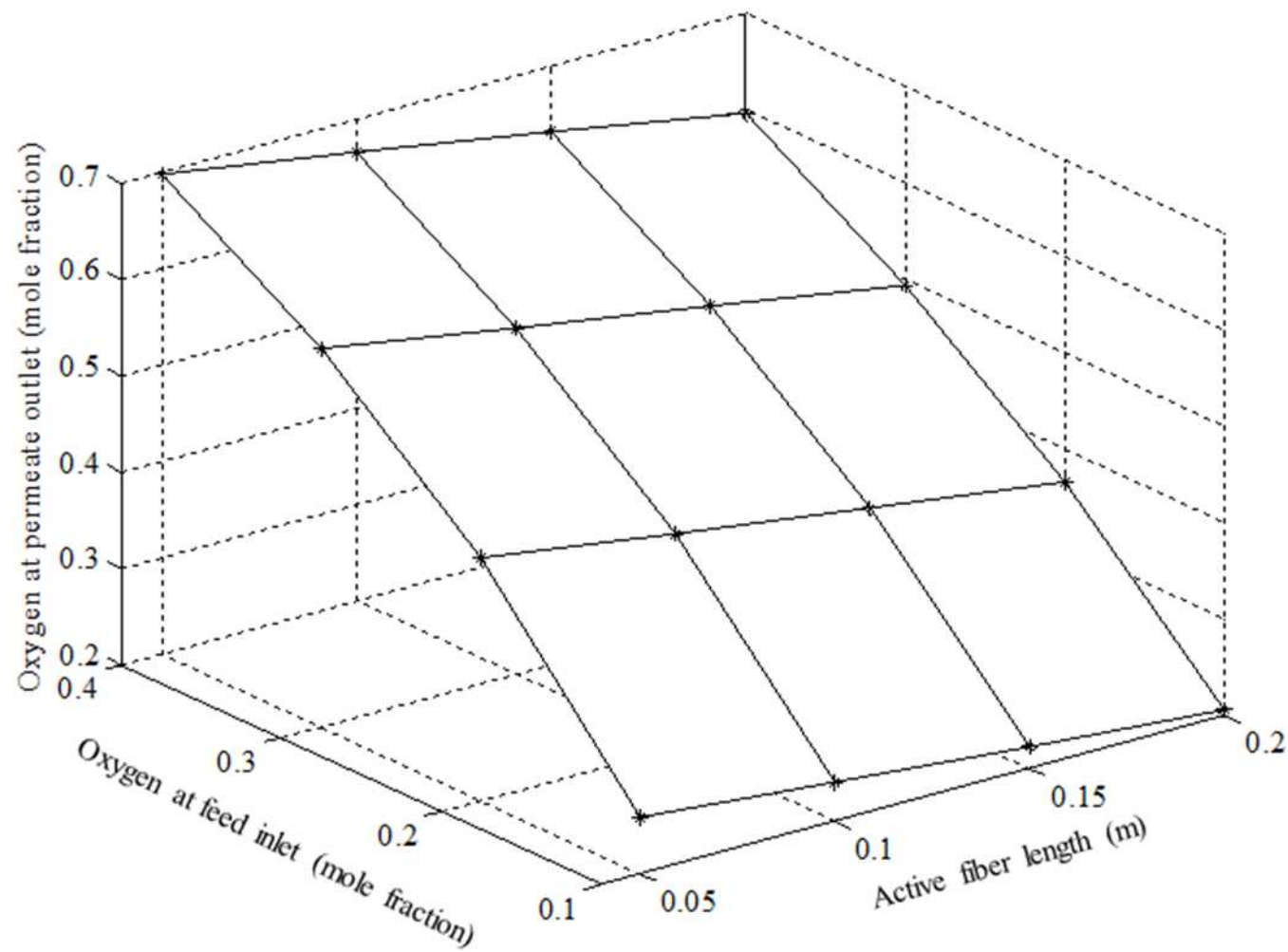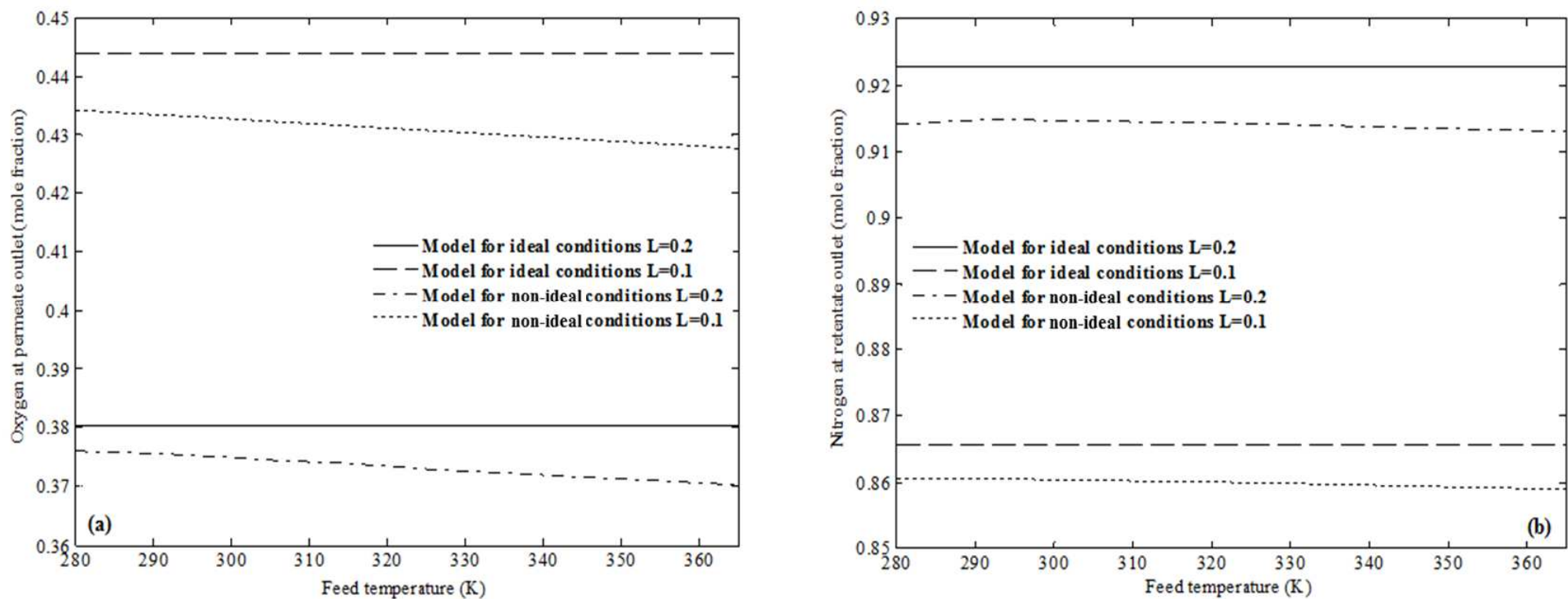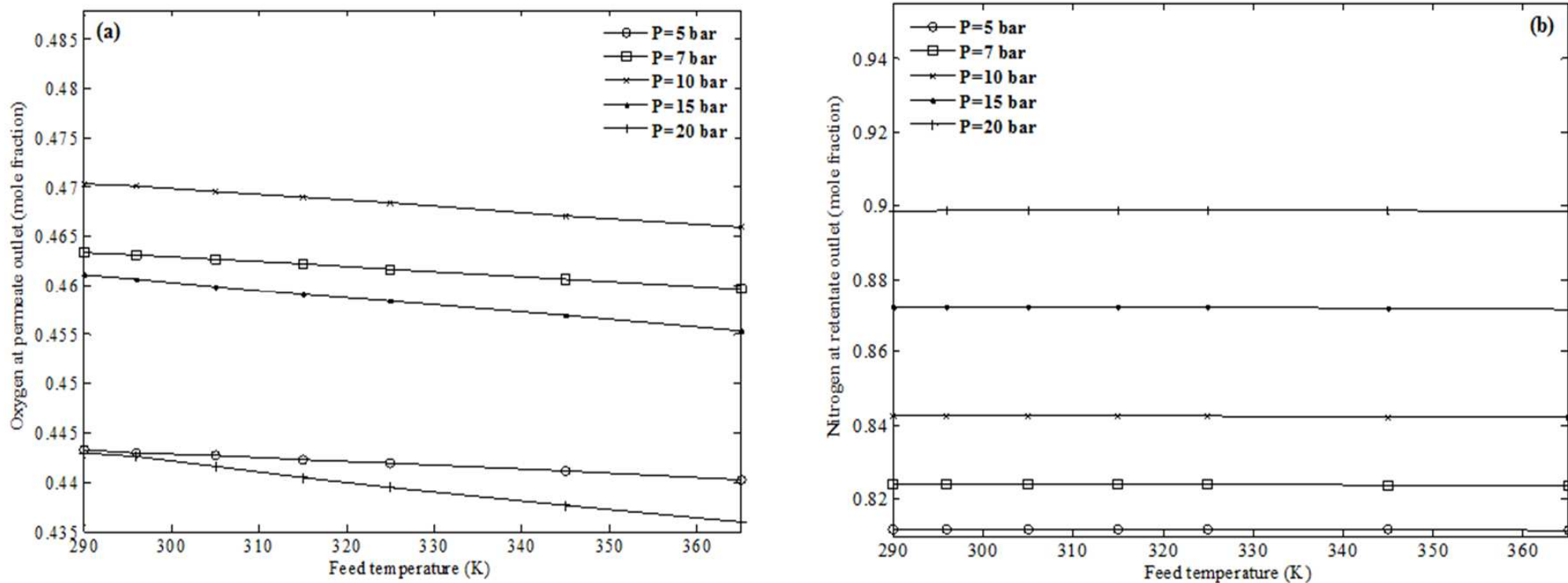**Figure 3.** The effect of active fiber length on the products purity at different feed compositions simulated using non-ideal model a) O_2 mole fraction in permeate outlet b) N_2 mole fraction in retentate outlet. (Testing conditions are provided in Table 1)
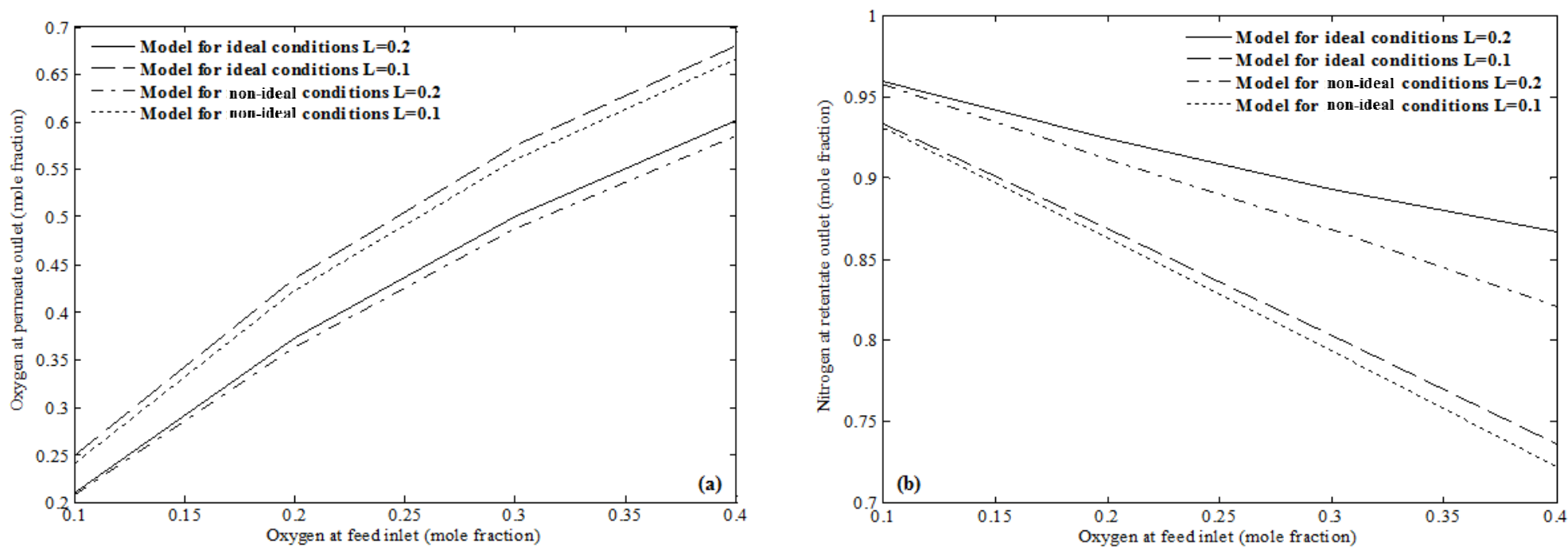
Figure 4. The effect of feed composition on the products purity a) O_2 mole fraction in outlet permeate stream b) N_2 mole fraction in outlet retentate stream. (Testing conditions are provided in Table 1)
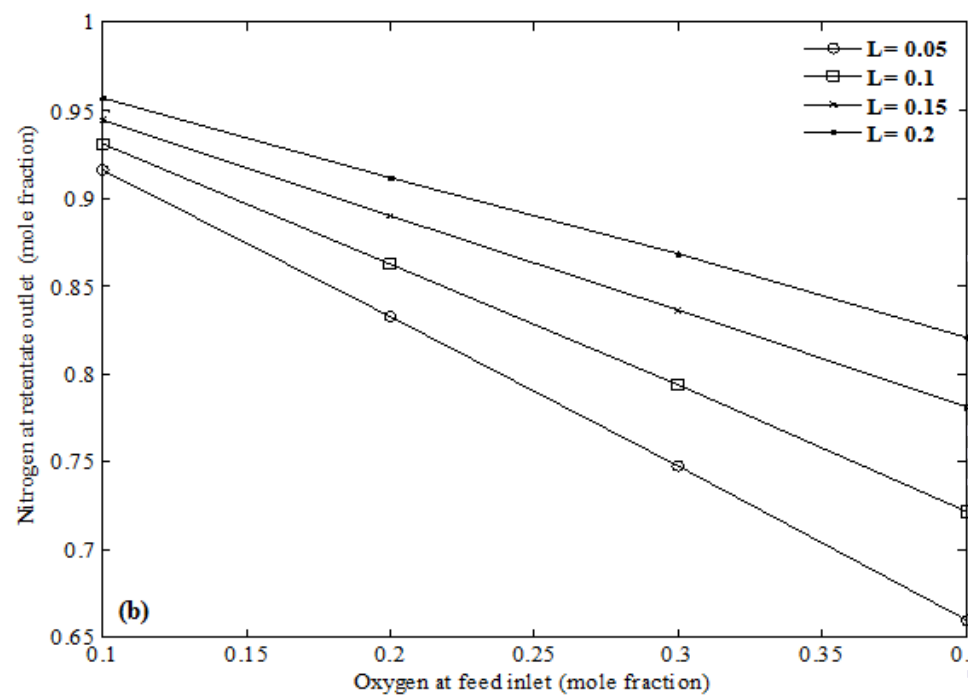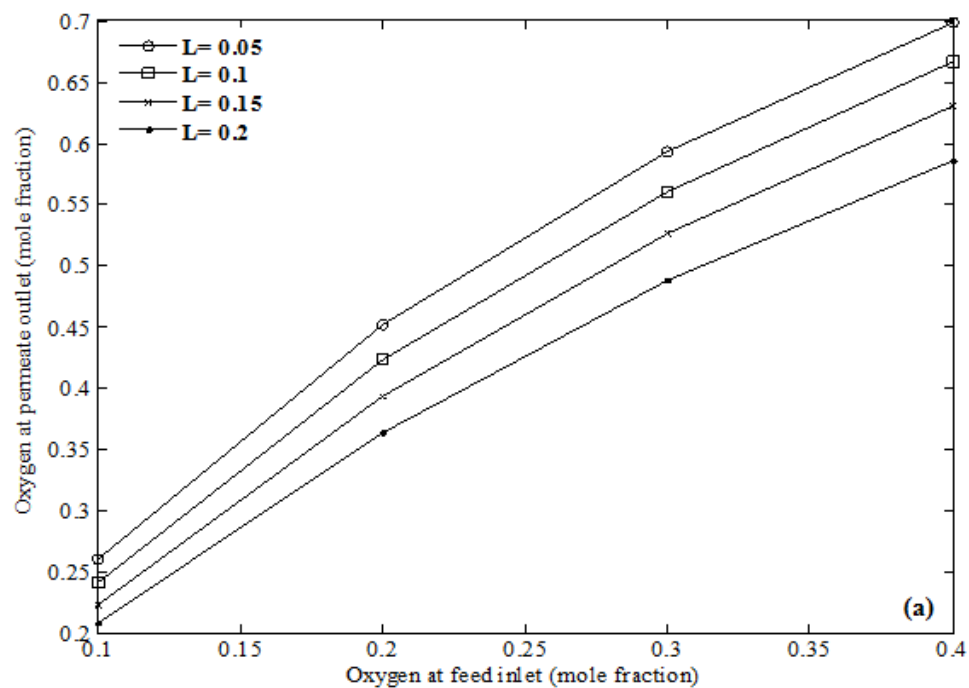
Figure 5. The effect of feed composition on the products purity at different length simulated using non-ideal model a) O_2 mole fraction in outlet permeate stream b) N_2 mole fraction in outlet retentate stream. (Testing conditions are provided in Table 1)
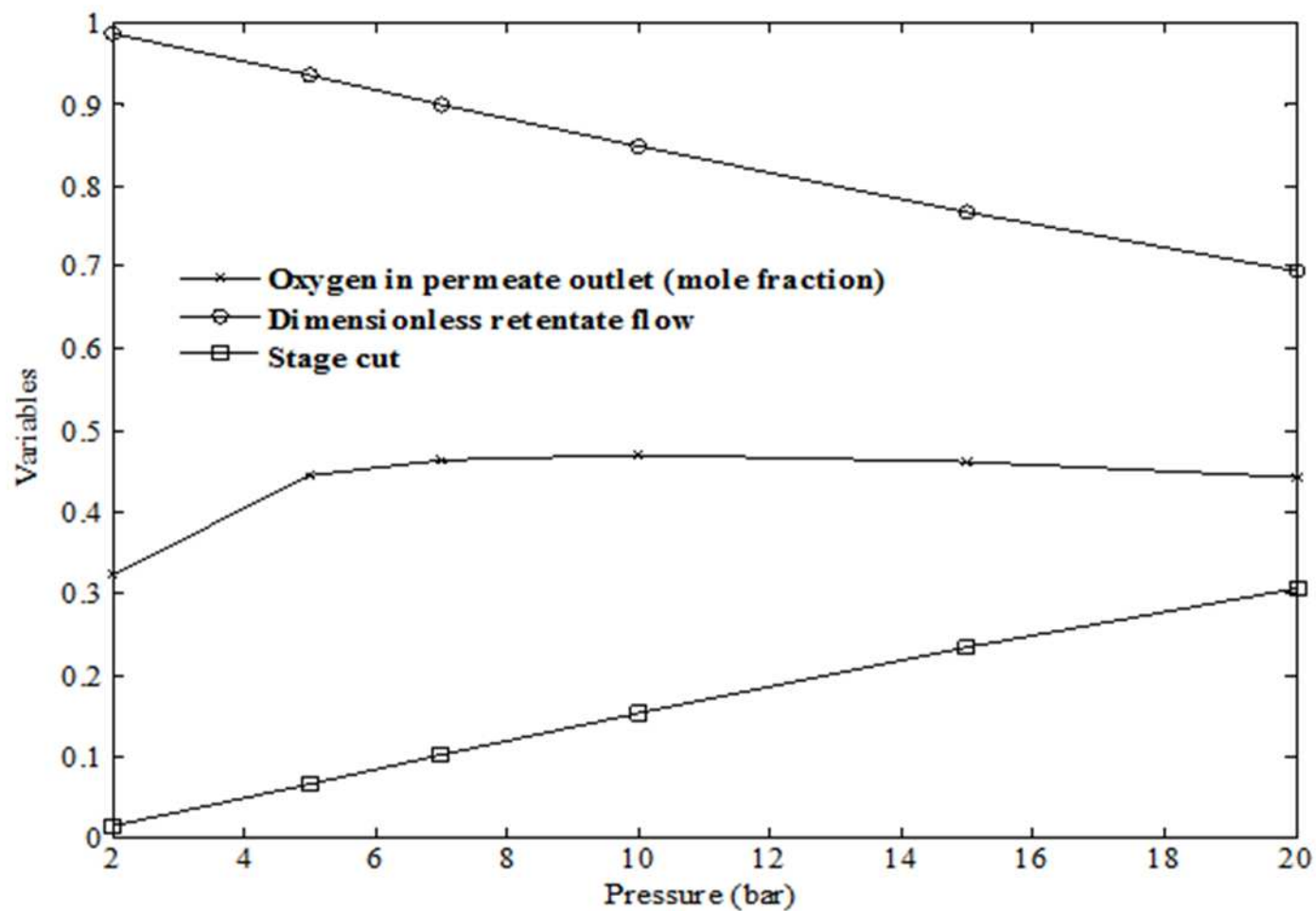
Figure 6. The effect of feed composition and fiber length on the oxygen purity simulated using non-ideal model. (Testing conditions are provided in Table 1)
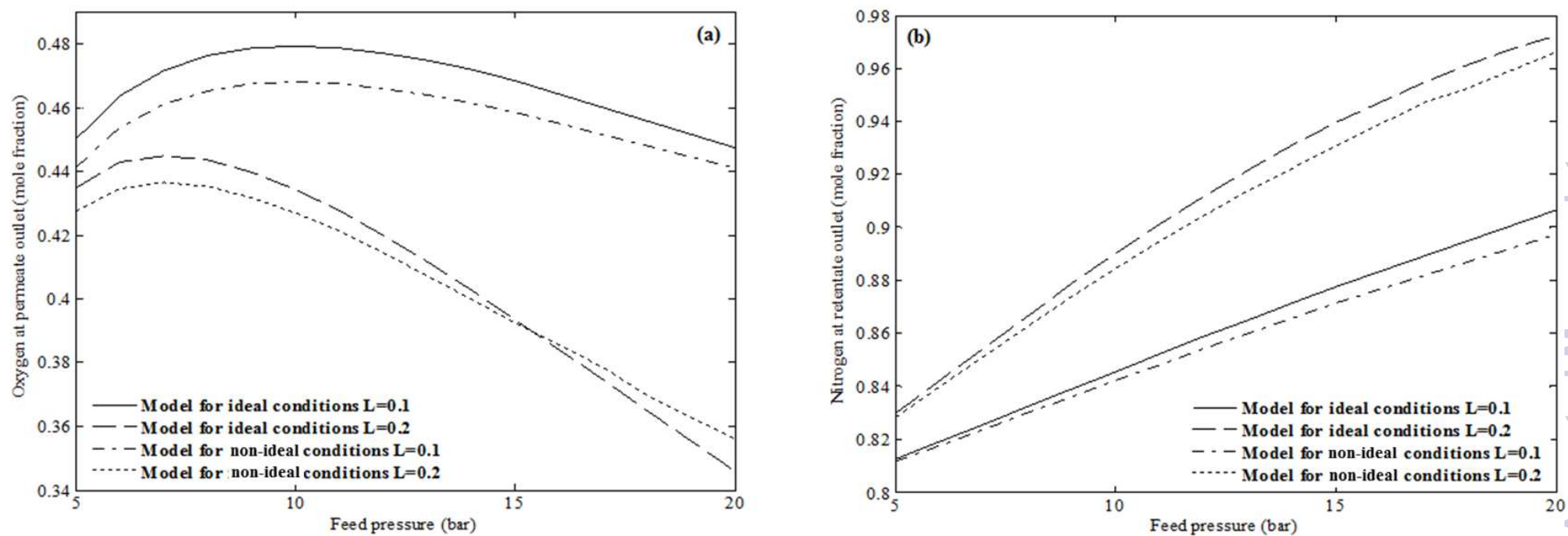
Figure 7. The effect of temperature on the products purity a) O_2 mole fraction in permeate stream b) N_2 mole fraction in retentate stream. (Testing conditions are provided in Table 1)
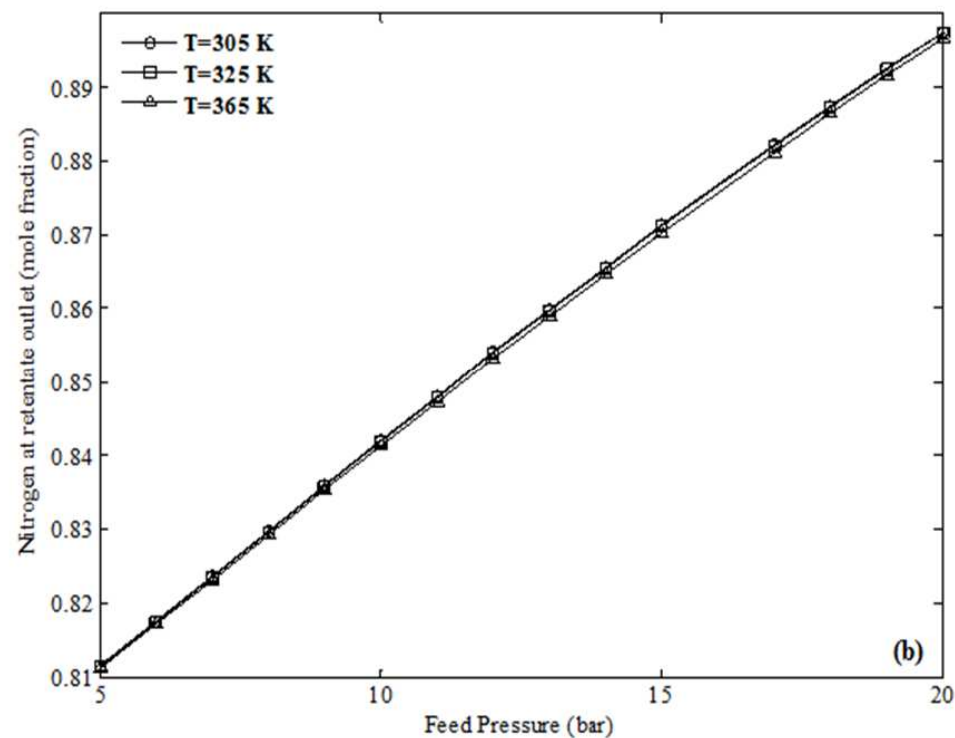
Figure 8. The effect of temperature on the products purity at different pressures simulated using non-ideal model a) O_2 mole fraction in permeate stream b) N_2 mole fraction in retentate stream. (Testing conditions are provided in Table 1)

Figure 9. The trends of oxygen purity, dimensionless retentate and stage cut as a function of pressure simulated using non-ideal model. (Testing conditions are provided in Table 1)

Figure 10. The effect of pressure on the products purity a) O_2 mole fraction in permeate stream b) N_2 mole fraction in retentate stream. (Testing conditions are provided in Table 1)
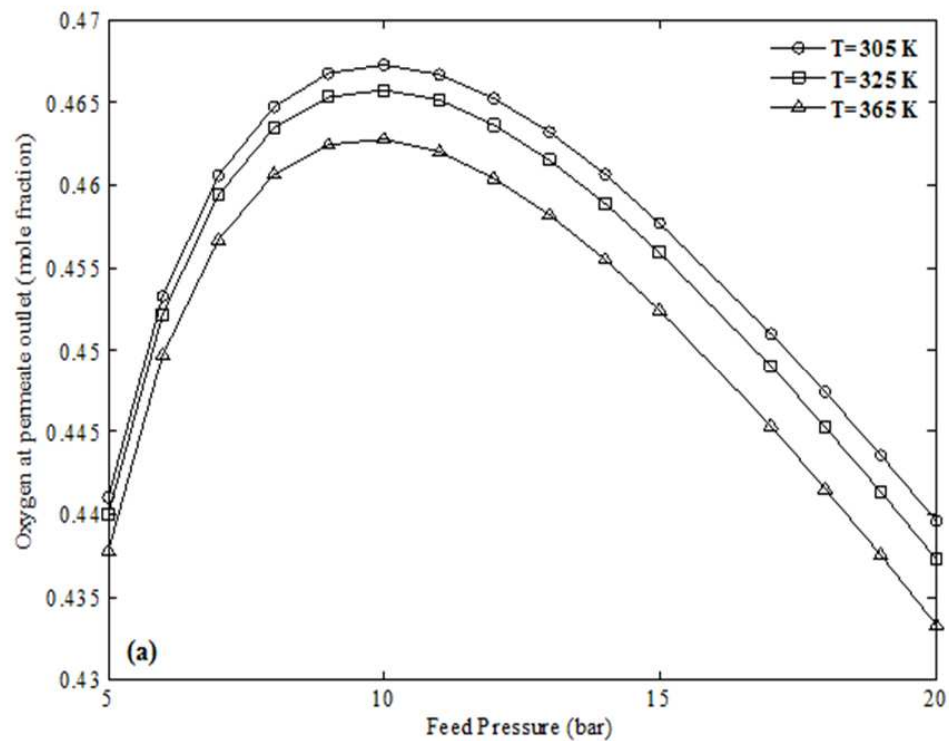
Figure 11. The effect of pressure on the products purity at different temperatures simulated using non-ideal model a) O_2 mole fraction in permeate stream b) N_2 mole fraction in retentate stream. (Testing conditions are provided in Table 1)
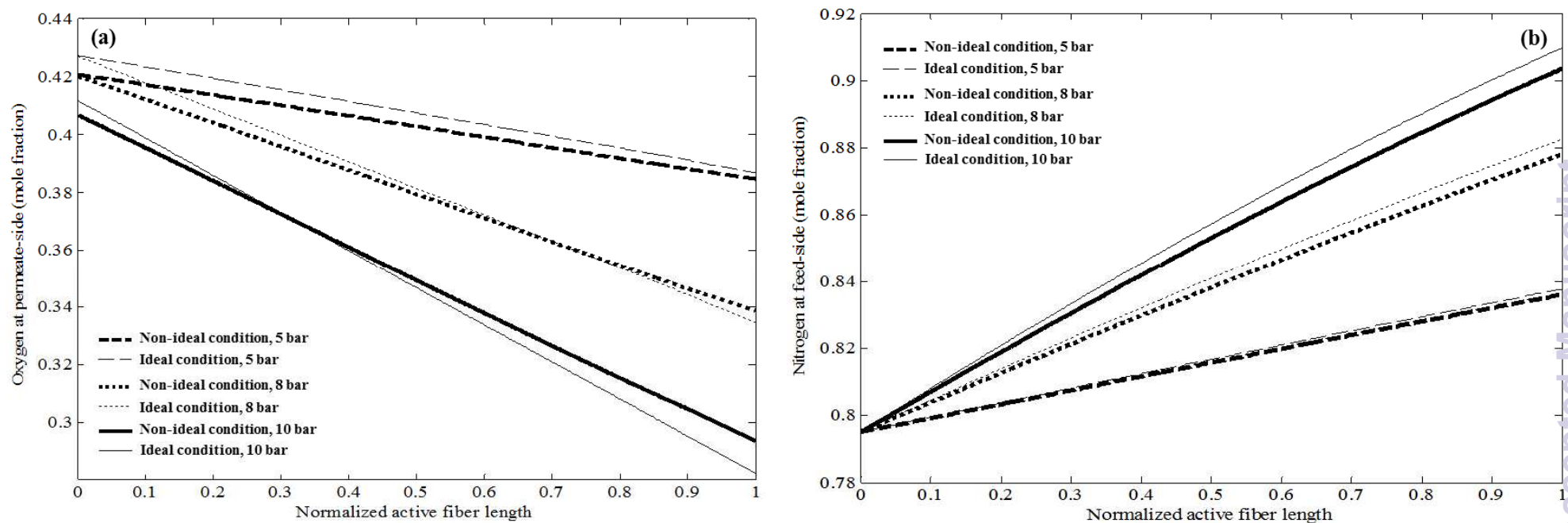
Figure 12. The effect of feed pressure on the mole fraction of components in a) O_2 mole fraction in permeate stream b) N_2 mole fraction in retentate stream (Testing conditions are provided in Table 1)
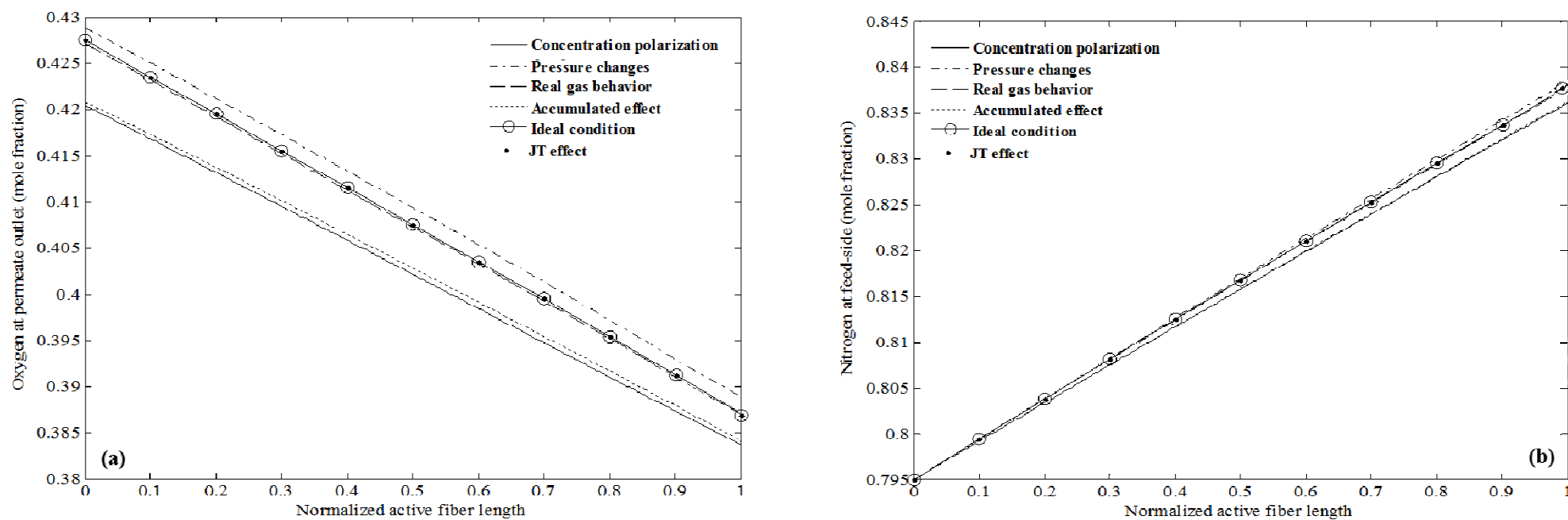
Figure 13. a) O$_2$ mole fraction in permeate-side stream b) N$_2$ mole fraction in feed-side stream along the active fiber length. The feed pressure is 5 bar. (Testing conditions are provided in Table 1, Associated parameters related to each non-ideal effect are provided in Table 2)

Figure 14. a) O$_2$ mole fraction in permeate-side stream b) N$_2$ mole fraction in feed-side stream along the active fiber length. The feed pressure is 8 bar. (Testing conditions are provided in Table 1, Associated parameters related to each non-ideal effect are provided in Table 2)
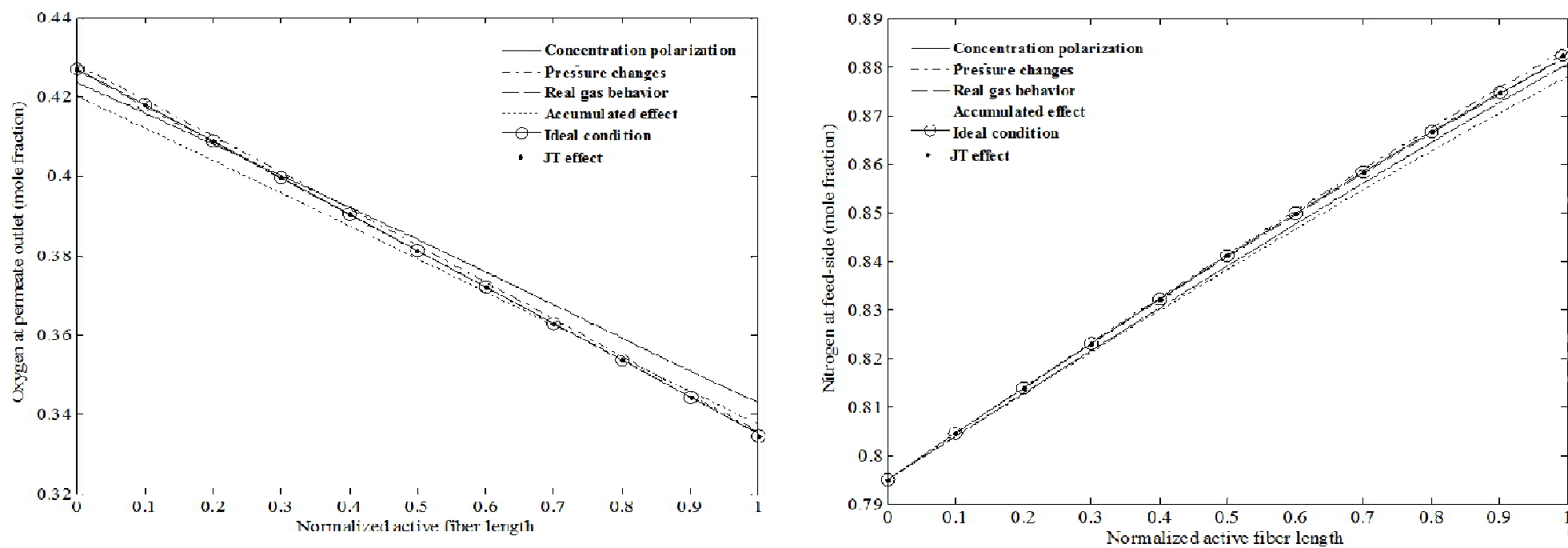
Figure 15. a) O_2 mole fraction in permeate-side stream b) N_2 mole fraction in feed-side stream along the active fiber length. The feed pressure is 10 bar. (Testing conditions are provided in Table 1, Associated parameters related to each non-ideal effect are provided in Table 2)
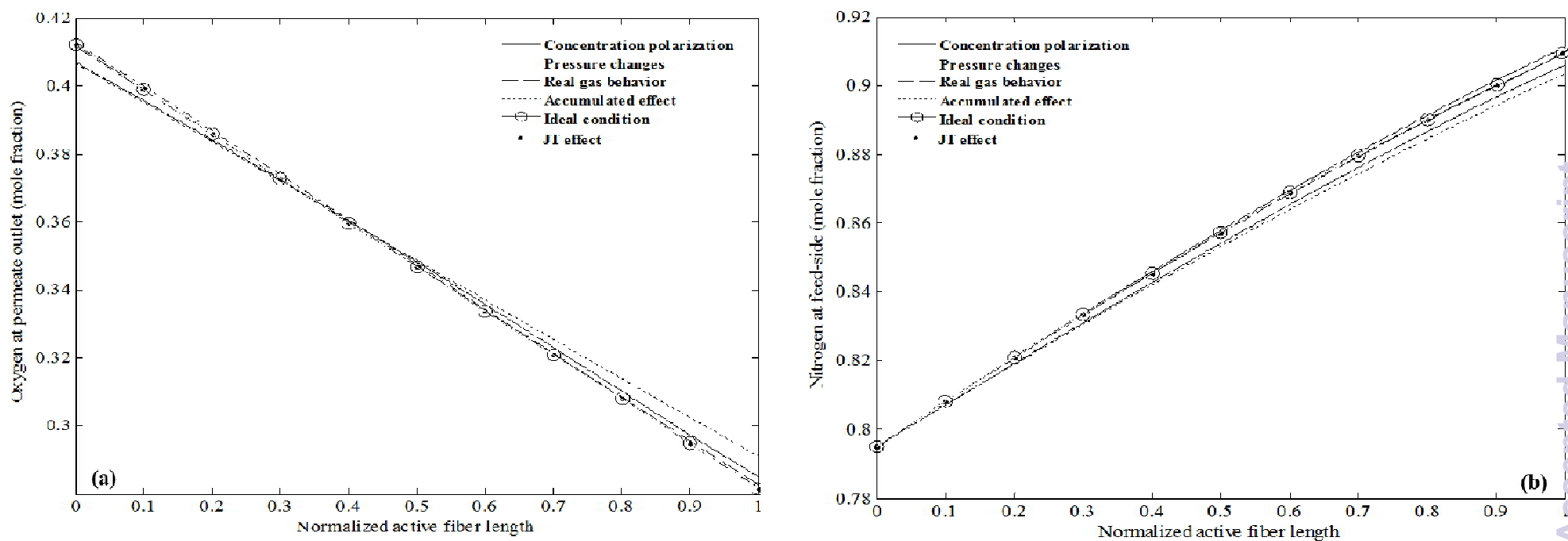
Table 1. Membrane module properties and operating conditions [32].

Parameter	Unit	Value
Inner fiber diameter	μm	80
Outer fiber diameter	μm	160
Module diameter	mm	9.5
Number of fibers	-	368
Active fiber length	cm	25
Feed mole fractions	-	0.205 O_2 0.795 N_2
Feed pressure	kPa	790.8
Permeate outlet pressure	kPa	101.3
Feed temperature	K	296.15
Permeance	$10^{-10} \frac{mol}{m^2.s.Pa}$	30.78 O_2 5.7 N_2
Activation energy for permeation	$\frac{kJ}{mol}$	19.3 O_2 27.6 N_2

Table 2. Parameters associated to the model considering non-ideal conditions.

Average of Parameters		P=5 bar	P=8 bar	P=10 bar
Fugacity coefficient in feed side	O_2	0.9972	0.9955	0.9944
	N_2	0.9997	0.9995	0.9994
Fugacity coefficient in permeate side	O_2	0.9994	0.9994	0.9994
	N_2	0.9999	0.9999	0.9999
Temperature drop across membrane		0.9501	1.6388	2.0856
Pressure loss in feed side		3.17e-7 bar	1.46e-7 bar	9.4e-8 bar
Pressure build-up in permeate side		0.0265 bar	0.0453 bar	0.0561 bar
Pressure drop across membrane		4.00 bar	7.02 bar	9.02 bar
Index of concentration polarization		0.0290	0.0425	0.0496
Reynolds number	Feed	2.5111	2.3380	2.2300
	Permeate	0.4994	0.8516	1.0551